

## Study of fragmentation at low excitation energies within a dynamical microscopic theory

Jatinder K. Dhawan and Rajeev K. Puri

*Physics Department, Panjab University, Chandigarh-160 014, India*

(Received 22 November 2006; published 10 May 2007)

We present the theoretical study of fragmentation at low excitation energies within dynamical microscopic theory namely, simulated annealing clusterization algorithm (SACA) and quantum molecular dynamics (QMD) model. For low excitation energy reactions, we choose the balance energies for a large number of reactions throughout the periodic table. We see that SACA gives multiplicities in terms of power law. For light fragments, it is close to  $1/3$ , whereas, for heavier fragments it is nearly mass independent suggesting their origin in terms of participant-spectator picture.

DOI: [10.1103/PhysRevC.75.057601](https://doi.org/10.1103/PhysRevC.75.057601)

PACS number(s): 25.70.Pq

The shattering of colliding nuclei into a large number of fragments is one of the hot topics in present day research. One is interested to know the cause of this breakup whether it is a statistical process, making microcanonical phase space model a proper tool or is it driven by the fluctuations during the collision [1–16].

By now, it is evident that this complex phenomenon depends crucially on several externally controlled parameters as well as on the internal model ingredients [1–16,18,20–23]. It also depends on the incident energy of the reaction and impact parameter (or colliding geometry) as well as on the mass of the system under investigation [8–10,15,20,23]. Further, dynamics driven by the asymmetric colliding nuclei ( $A_1 \gg A_2$ ;  $A_i$  are either projectile or target) are quite different compared to that of symmetric colliding nuclei ( $A_1 \simeq A_2$ ). At the same time, the equation of state, nucleonic cross sections, the density profiles of colliding nuclei, momentum dependence of the equation of state, and Gaussian width of nucleons have also been reported to have a sizable effect on the formation of fragments [22,23]. When, one talks about the multifragmentation via dynamical semiclassical transport models, one has to make sure that the quantum thermodynamical properties are properly implemented. This and other related questions are of no relevance if one has a reaction with high excitation energy. This is truly valid for central reactions at higher incident energies. However, these implementations may play an important role in reactions with low excitation energies.

As has been stated by many authors [8,11,14,18,21–23] no semiclassical dynamical model like the quantum molecular dynamics (QMD) model [18] or Boltzmann-Uehling-Uhlenbeck (BUU) model [17], simulates the fragments directly. Instead, the phase space of nucleons has to be clusterized at some stage of the reaction. The simplest approach was to look for the spatial distance of nucleons and if they are closer than some distance, e.g., 4 fm, they were supposed to form a fragment. Using this technique, the QMD model could not succeed in describing the data [20,26]. This failure led to the development of new clusterization methods based on the Metropolis technique [25,26]. Our new method was dubbed as the simulated annealing clusterization algorithm (SACA) [26]. This method was able to explain the experimental findings at low excitation energy which is typical either in low incident

energy reactions or in spectator matter breakups. Based on the same technique, we plan to apply this new method SACA to low energy symmetric reactions throughout the periodic table for the first time. Most of the earlier attempts have been constrained to high excitation energies range. Further, this is the first ever attempt to robust SACA over an entire mass range varying between 63 and 394. Rather than taking a fixed incident energy, we look for a more meaningful energy spectrum. It has been argued in the literature that the interactions at low incident energies are dominated by the attractive mean field whereas repulsive nucleon-nucleon scatterings take a lead at higher incident energies. While going from low to high incident energy, these interactions are balanced at a particular point. This energy point has also been termed as balance energy  $E_{\text{bal}}$  [24,27–32]. We plan to address the question of fragmentation at this balance point within microscopic theory.

For this analysis, we employ the quantum molecular dynamics (QMD) model. The reader is referred to Ref. [18] for details. The clusterization is done within the simulated annealing clusterization algorithm (SACA).

In this approach [26], a group of nucleons can form a fragment if the total fragment energy/nucleon  $\zeta_i$  is below a minimum binding energy:

$$\zeta_i = \frac{1}{N_f} \sum_{i=1}^{N_f} \left[ \sqrt{(P_i - P_{N_f}^{\text{c.m.}})^2 + m_i^2} - m_i + \frac{1}{2} \sum_{i=1}^{N_f} V_{ij}(r_i, r_j) \right] < E_{\text{bind}}. \quad (1)$$

We take  $E_{\text{bind}} = -4.0$  MeV if  $N^f \geq 3$  and  $E_{\text{bind}} = 0$  otherwise. In this equation,  $N^f$  is the number of nucleons in a fragment,  $P_{N_f}^{\text{c.m.}}$  is the center-of-mass momentum of the fragment.

To find the most bound configuration, we start with a random configuration. The energy of the individual clusters is calculated using Eq. (1). Let the total energy of a configuration  $k$  be  $E_k (= \sum_i N_f \zeta_i)$ , where  $N_f$  is the number of nucleons in a fragment  $i$  and  $\zeta_i$  is the energy per nucleon associated with the fragment  $i$ . Suppose a new configuration  $k'$  [which is obtained

by (a) transferring a nucleon from some randomly chosen fragment to another fragment, by (b) setting a nucleon free, or by (c) absorbing a free nucleon into a fragment] has total energy  $E'_k$ . If the energy difference between the old and new energy,  $\Delta E (= E'_k - E_k)$ , is negative, the new configuration is always accepted. If not, the new configuration  $k'$  may nevertheless be accepted with a probability of  $\exp(-\Delta E/c)$ , where  $c$  is called the control parameter. The control parameter is decreased in small steps. This algorithm will yield eventually the most bound configuration (MBC).

In the present study, we used a stiff equation of state along with 40 mb nucleon-nucleon cross section. This combination was found to reproduce the balance energies for over 15 reactions very closely [24]. We simulated each of reactions  $^{36}\text{Ar}+^{27}\text{Al}$  ( $b = 2$  fm),  $^{40}\text{Ar}+^{27}\text{Al}$  ( $b = 1.6$  fm),  $^{40}\text{Ar}+^{45}\text{Sc}$  ( $b/b_{\text{max}} = 0.4$ ),  $^{40}\text{Ar}+^{51}\text{V}$  ( $b/b_{\text{max}} = 0.3$ ),  $^{64}\text{Zn}+^{48}\text{Ti}$  ( $b = 2$  fm),  $^{58}\text{Ni}+^{58}\text{Ni}$  ( $b/b_{\text{max}} = 0.28$ ),  $^{64}\text{Zn}+^{58}\text{Ni}$  ( $b = 2$  fm),  $^{86}\text{Kr}+^{93}\text{Nb}$  ( $b/b_{\text{max}} = 0.4$ ),  $^{93}\text{Nb}+^{93}\text{Nb}$  ( $b/b_{\text{max}} = 0.3$ ),  $^{139}\text{La}+^{139}\text{La}$  ( $b/b_{\text{max}} = 0.3$ ), and  $^{197}\text{Au}+^{197}\text{Au}$  ( $b = 2.5$  fm) for 1000–3000 events. The impact parameter is guided by the experimental measurements. The incident energies used in the above reactions are the balance energies taken from Ref. [24]. These read, respectively, as 74, 67.3, 89.4, 67.8, 59.3, 62.6, 56.6, 69.2, 57, 51.6, and 43 MeV/nucleon. The phase space, thus obtained, was subjected to clusterization using the SACA algorithm. Recently, SACA was also applied to the reaction of  $^{197}\text{Au}+^{197}\text{Au}$  at 35 MeV/nucleon for impact parameters  $b/b_{\text{max}}$  between 0.5 and 0.9. A very close agreement was obtained for the mass yields between QMD+SACA and experimental data [33]. Note that at such a low incident energy and peripheral collisions, a perfect low excitation energy spectator matter physics is obtained.

Let us first examine the phase space at the balance point. In Fig. 1, we display the result of a single event in the  $(x, z)$

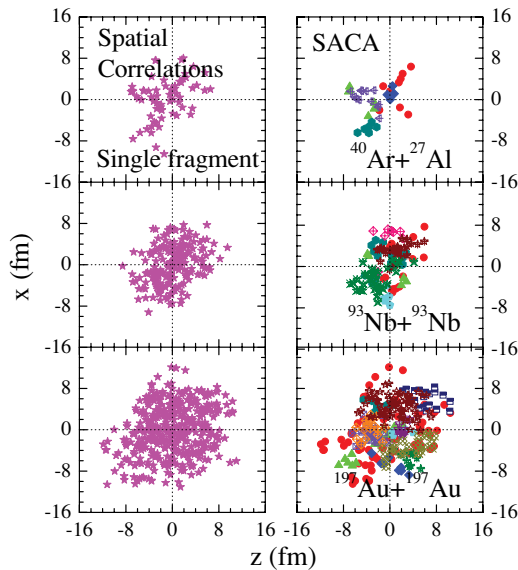


FIG. 1. (Color online) The snapshots of a single event in the coordinate space  $(x, z)$ . The left side is for the spatial correlation method whereas results from SACA are displayed on right side. The graph is at the time when heaviest fragment in SACA has a minimal value.

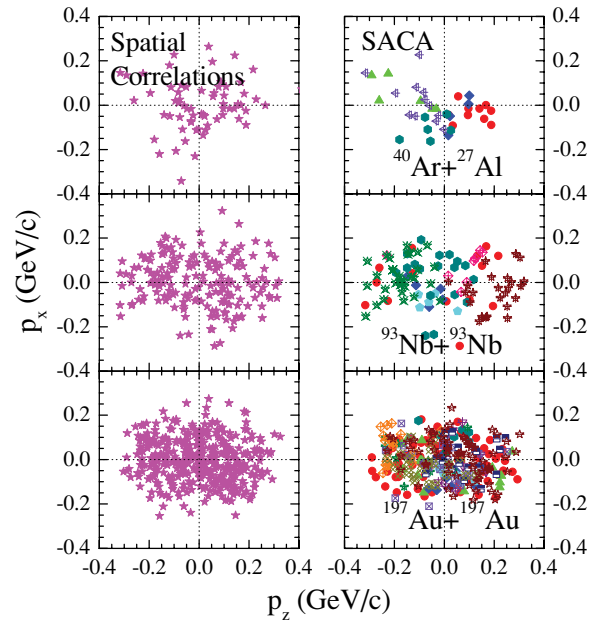


FIG. 2. (Color online) Same as Fig. 1, but in the momentum space.

plane whereas the same event is shown in  $(p_x, p_z)$  plane in Fig. 2. We show the reactions of  $^{40}\text{Ar}+^{27}\text{Al}$ ,  $^{93}\text{Nb}+^{93}\text{Nb}$ , and  $^{197}\text{Au}+^{197}\text{Au}$  at their corresponding theoretical balance energies to cover the entire mass range. As noted in Ref. [26], the true fragmentation is supposed to occur at a time when the heaviest fragment has a minimal value. This time of fragmentation varies with the incident energy and mass of colliding partners. Here, we also display a single fragment obtained in the spatial method. The same fragment was then subjected to the SACA technique. We see that the big fragment obtained with the spatial correlation method is indeed not a single fragment. Instead, it is a group of several overlapping fragments. Since, these fragments share the same space, they appear to be a single fragment. Once SACA is applied, one sees clearly that this single fragment is a bundle of fragments. As seen in the SACA, these fragments are indeed a cluster of overlapping fragments whose nucleons continue to interact with the surroundings. While looking at Fig. 2, it is immediately clear that although different fragments overlap in spatial space, they all have distinct momentum spaces and hence are properly bound. We have also checked the binding energy of all the fragments detected in the SACA method. These fragments are properly bound. Due to lower balance energy in the  $^{197}\text{Au}+^{197}\text{Au}$  reaction, a smaller phase-space is opened up for the binary nucleon-nucleon collisions, causing the Pauli-principle to play a dominant role. This role is reduced for the lighter colliding nuclei having higher balance energy.

In Fig. 3, we display the time evolution of  $A^{\text{max}}$ , Free nucleons,  $2 \leq A \leq 4$  (LMF's) as well as  $5 \leq A \leq 30\%$  (IMF's) at the energy of vanishing flow. Here 30% is the 30% of the mass of the larger nuclei among target and projectile. As evident from the figure, largest fragment ( $A^{\text{max}}$ ) passes through a minimum value which increases at a later time due to the reabsorption of fragments. The emission of free nucleons ( $A = 1$ ), LMF's and IMF's starts around 30 fm/c.

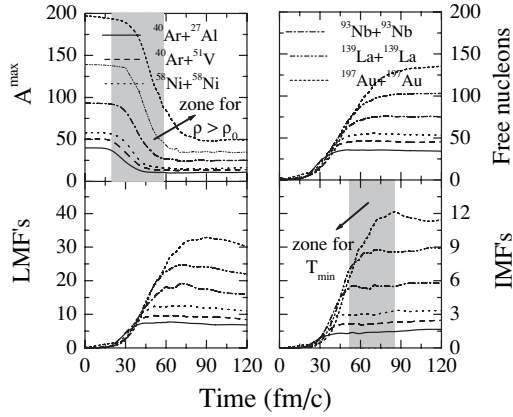


FIG. 3. The time evolution of  $A^{\max}$ , free nucleons, LMF's and IMF's for the reactions of  $^{40}\text{Ar}+^{27}\text{Al}$ ,  $^{40}\text{Ar}+^{51}\text{V}$ ,  $^{58}\text{Ni}+^{58}\text{Ni}$ ,  $^{93}\text{Nb}+^{93}\text{Nb}$ ,  $^{139}\text{La}+^{139}\text{La}$ , and  $^{197}\text{Au}+^{197}\text{Au}$  at their balance energy, respectively. We also display the zones for high density and also the time of true fragment pattern for all the reactions listed in the text.

It is also evident that the reaction with lighter colliding nuclei saturates much faster compared to heavy nuclei. This is due to the fact that the balance energy in heavier nuclei is much smaller compared to lighter nuclei. All the fragments are quite stable. Their stability can also be checked via a persistence coefficient which is also found to be quite stable. We have also shown the zones for high density and also the time of true fragmentation. We noticed that the fragment pattern is visible just after the phase of high density.

In Fig. 4, we plot the  $A^{\max}$ ,  $Z^{\max}$ , multiplicity of free nucleons, LMF's,  $5 \leq A \leq 9$  (MMF's),  $2 \leq A \leq 30\%$ , and IMF's,

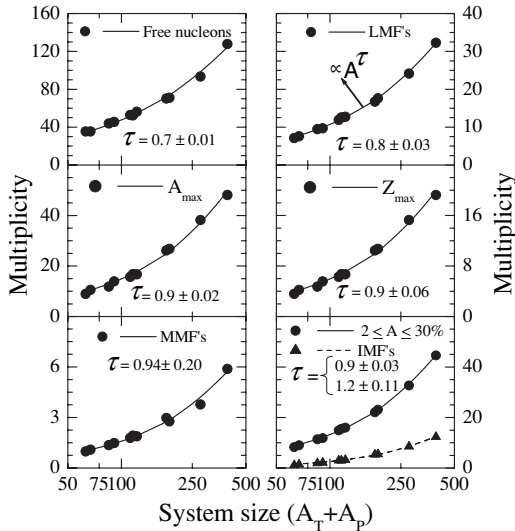


FIG. 4.  $A^{\max}$ ,  $Z^{\max}$ , and multiplicities of free nucleons,  $2 \leq A \leq 4$  (LMF's) and  $5 \leq A \leq 9$ ,  $2 \leq A \leq 30\%$ , and  $5 \leq A \leq 30\%$  (IMF's) as a function of composite mass of the colliding nuclei ( $A_T + A_P$ ) for the reactions of  $^{36}\text{Ar}+^{27}\text{Al}$ ,  $^{40}\text{Ar}+^{27}\text{Al}$ ,  $^{40}\text{Ar}+^{45}\text{Sc}$ ,  $^{40}\text{Ar}+^{51}\text{V}$ ,  $^{64}\text{Zn}+^{48}\text{Ti}$ ,  $^{58}\text{Ni}+^{58}\text{Ni}$ ,  $^{64}\text{Zn}+^{58}\text{Ni}$ ,  $^{86}\text{Kr}+^{93}\text{Nb}$ ,  $^{93}\text{Nb}+^{93}\text{Nb}$ ,  $^{139}\text{La}+^{139}\text{La}$ , and  $^{197}\text{Au}+^{197}\text{Au}$  at their theoretical balance energies, respectively. The power law fits ( $\propto A^\tau$ ) are also displayed as solid lines.

respectively, as a function of the mass of the system. All these multiplicities of different fragments follow a linear power law  $\propto A^\tau$ . A similar mass power law was also obtained using the spatial correlation method [34]. There, all these fragments were reported to follow a power factor close to 1/3 which is similar to that obtained for the balance energy. In contrary, using microscopic SACA, we obtained different dependence for different fragments. If we rescale the multiplicities with system size, the power factor is close to 1/3 for free nucleons and LMF's. Whereas it is nearly mass independent for other fragments like largest fragment ( $A^{\max}$ ), charge ( $Z^{\max}$ ), medium mass fragments ( $5 \leq A \leq 9$ ) and different forms of IMF's. The primary cause of the difference between spatial and SACA analysis emerges due to fact that SACA can identify the fragments even if they are overlapping. This property of SACA leads to more fragments compared to the spatial correlation method. This effect is more pronounced for a heavier system like  $^{197}\text{Au}+^{197}\text{Au}$  that has a smaller balance energy compared to a light system like  $^{12}\text{C}+^{12}\text{C}$  where balance energy is quite high. Naturally, with an increase in incident energy (and excitation energy), more phase space is opened for binary collisions and hence fragments are well separated. These fragments can be safely detected by the spatial correlation method. We have tested that both algorithms reach asymptotic values after 1000–1200 fm/c at higher incident energies. The time taken at low incident energies is, however, very long. Since we also have to be careful about the stability of nuclei, we had to stop the calculation at 1000 fm/c in the MST method. This has no effect for lighter nuclei where  $E_{\text{bal}}$  is quite large. For the case of heavy nuclei (like  $^{197}\text{Au}+^{197}\text{Au}$ ),  $E_{\text{bal}}$  is very low, therefore, their fragment pattern with the MST method may be premature. The mass independent nature of the heavier fragments can also be coupled with our recent observation of the mass independent nature of participant-spectator matter at the energy of vanishing flow. This mass independent nature was related to the counterbalancing of attractive and repulsive forces. The nearly 1/3 dependence in free nucleons and LMF's is related with the fact that light complex particles are produced as a coalescence of phase-space which has attractive surface and repulsive scattering terms, therefore leading to 1/3 dependence.

In summary, we have studied the fragmentation at the energy of disappearance of flow where the excitation energy is very small and spectator-matter decay physics dominate. This was done within the framework of the simulated annealing clusterization algorithm (SACA). For all the systems studied here (between mass 63 and 394), the largest fragment passes through a minimum value which increases at a later time due to the reabsorption of fragments. The study of multifragmentation at balance energy reveals a linear power law. The power factor, however, varies with the different fragments. It is close to 1/3 for lighter fragments like free nucleons and LMF's whereas it is mass independent for medium and intermediate mass fragments which could be understood in terms of participant-spectator matter picture.

Work supported by CSIR, Government of India via Grant no. 03(1078)/06/EMR-II, India.

- [1] B. Jakobsson *et al.*, Nucl. Phys. **A509**, 195 (1990); H. W. Barz *et al.*, *ibid.* **A548**, 427 (1992).
- [2] J. Colin *et al.*, Phys. Rev. C **67**, 064603 (2003).
- [3] B. K. Srivastava *et al.*, Phys. Rev. C **65**, 054617 (2002).
- [4] R. P. Scharenberg *et al.*, Phys. Rev. C **64**, 054602 (2001).
- [5] S. Hudan *et al.*, Phys. Rev. C **67**, 064613 (2003).
- [6] J. P. Bondorf, A. S. Botvina, and I. N. Mishustin, Phys. Rev. C **58**, R27 (1998).
- [7] J. Pochodzalla *et al.*, Nucl. Phys. **A583**, 553 (1995).
- [8] Y. G. Ma and W. Q. Shen, Phys. Rev. C **51**, 710 (1995).
- [9] A. Schuttauf *et al.*, Nucl. Phys. **A607**, 457 (1996); J. P. Hubbele *et al.*, Z. Phys. A **340**, 263 (1991).
- [10] N. T. B. Stone *et al.*, Phys. Rev. Lett. **78**, 2084 (1997).
- [11] D. Sisan *et al.*, Phys. Rev. C **63**, 027602 (2001).
- [12] N. Marie *et al.*, Phys. Lett. **B391**, 15 (1997); R. Wada *et al.*, Phys. Rev. C **55**, 227 (1997); D. Dore *et al.*, *ibid.* **63**, 034612 (2001).
- [13] L. Phair *et al.*, Phys. Rev. Lett. **75**, 213 (1995); T. C. Sangster *et al.*, Phys. Rev. C **46**, 1404 (1992).
- [14] A. Bohnet *et al.*, Nucl. Phys. **A494**, 349 (1989).
- [15] C. A. Oglivie *et al.*, Phys. Rev. C **42**, R10 (1990).
- [16] R. Donangelo, H. Schulz, K. Sneppen, and S. R. Souza, Phys. Rev. C **50**, R563 (1994); C. Williams *et al.*, *ibid.* **55**, R2132 (1997).
- [17] G. F. Bertsch and S. Das Gupta, Phys. Rep. **160**, 189 (1988); W. Bauer, Phys. Rev. Lett. **61**, 2534 (1988).
- [18] J. Aichelin, Phys. Rep. **202**, 233 (1991).
- [19] H. Stöcker and W. Griener, Phys. Rep. **137**, 277 (1986).
- [20] M. Begemann-Blaich *et al.*, Phys. Rev. C **48**, 610 (1993); M. B. Tsang *et al.*, Phys. Rev. Lett. **71**, 1502 (1993).
- [21] R. K. Puri and S. Kumar, Phys. Rev. C **57**, 2744 (1998).
- [22] C. Hartnack, R. K. Puri, J. Aichelin, J. Konopka, S. A. Bass, H. Stöcker, and W. Greiner, Eur. Phys. J. A **1**, 151 (1998).
- [23] J. Singh, S. Kumar, and R. K. Puri, Phys. Rev. C **62**, 044617 (2000).
- [24] A. D. Sood and R. K. Puri, Phys. Rev. C **69**, 054612 (2004).
- [25] C. Dorso and J. Randrup, Phys. Lett. **B301**, 328 (1993); N. Sator, Phys. Rep. **376**, 1 (2003).
- [26] R. K. Puri, C. Hartnack, and J. Aichelin, Phys. Rev. C **54**, R28 (1996); J. Singh and R. K. Puri, J. Phys. G: Nucl. Part. Phys. **27**, 2091 (2001).
- [27] D. J. Magestro, W. Bauer, and G. D. Westfall, Phys. Rev. C **62**, 041603(R) (2000).
- [28] D. Krofcheck *et al.*, Phys. Rev. C **43**, 350 (1991).
- [29] W. M. Zhang *et al.*, Phys. Rev. C **42**, R491 (1990); P. Crochet *et al.*, Nucl. Phys. **A624**, 755 (1997).
- [30] B. A. Li, Phys. Rev. C **48**, 2415 (1993).
- [31] V. de la Mota, F. Sebille, M. Farine, B. Remaud, and P. Schuck, Phys. Rev. C **46**, 677 (1992).
- [32] H. Zhou, Z. Li, Y. Zhuo, and G. Mao, Nucl. Phys. **A580**, 627 (1994).
- [33] J. Dhawan, private communication.
- [34] J. K. Dhawan and R. K. Puri, Phys. Rev. C **74**, 054610 (2006).